

Structural stability and equation of state of simple-hexagonal phosphorus to 280 GPa: Phase transition at 262 GPa

Yuichi Akahama and Haruki Kawamura

Department of Material Science, Faculty of Science, Himeji Institute of Technology, 1475-2 Kanaji, Kamigohri, Hyogo 678-1297, Japan

Stefan Carlson, Tristan Le Bihan, and Daniel Häusermann

High Pressure Experiment Division, European Synchrotron Radiation Facility, Boîte Postale 220, F-38043 Grenoble Cedex, France

(Received 22 February 1999)

A structural phase transition and the equation of state of the simple-hexagonal (sh) phase, P - V , of phosphorus were investigated at pressures up to 280 GPa using monochromatic synchrotron x-ray diffraction. The P - V phase, which was stable above 137 GPa, has shown a structural transition to a higher-pressure phase, P - VI , above 262 GPa, while the c/a ratio of the sh phase slightly increased with increasing pressure from 0.948 to 0.956. The structure of the P - VI phase has been proposed to be bcc. The bulk modulus (B_0) and the atomic volume at atmospheric pressure (V_0) of the sh phase were estimated to be 84.1 GPa and 14.2 \AA^3 , with a fixed value of the pressure derivative of the bulk modulus (B'_0).

I. Introduction. Phosphorus of the group-Vb elements exhibits a unique sequence of structural phase transitions under pressure.¹⁻³ At 4.5 GPa, black phosphorus, which is the most stable form with the A17 structure ($Cmca:P$ -I) at ambient conditions, undergoes a structural transition to the A7 phase ($R\bar{3}m:P$ -II)^{1,2} with a semiconductor-(semi)metal transition.^{4,5} The A7 phase transforms to the simple cubic (sc) phase ($Pm\bar{3}m:P$ -III) at 10 GPa.^{1,2} The sc phase behaves as a metal with a superconducting transition temperature of about 10 K.^{6,7} Recent structural studies have revealed that the sc phase transforms to the simple-hexagonal (sh) phase ($P6/mmm:P$ -V) at 137 GPa via an intermediate phase (unknown: P -IV).³ The fundamental transition from the sc to sh structure, which is the first observation in the monoatomic system, was accompanied by a relatively large volume reduction of 7.6% due to the result of an increase in the coordination number from 6 to 8.

The sh structure is rare in the Periodic Table and reported only in the high-pressure phase of Si (Refs. 8 and 9) and Ge.¹⁰ A special feature of the structure is its lower packing fraction of atoms, 0.605, compared with the bcc (0.680) and the fcc (0.740) or hcp structures. The sh phases of Si and Ge transform to the hcp structure^{8,10} via an intermediate orthorhombic phase¹¹ and for Si, further to the fcc structure.¹² Therefore, a structural transition to a structure with the higher packing fraction such as bcc, hcp or fcc has been expected.³ We have performed a high-pressure powder x-ray-diffraction experiment on phosphorus in an extremely high-pressure region near 300 GPa in order to determine the equation of state of the sh phase and research the expected structural transition. On the other hand, there are several theoretical studies¹³⁻¹⁵ on the structural stability of phosphorus under pressure but only one report by Sasaki *et al.*¹⁵ has predicted a sc to bcc transition at 135 GPa.

In this paper, we report the observation of a new structural transition from the sh phase to the P - VI phase at 262 GPa and propose the bcc structure for the P - VI phase. The transition pressure is the highest one for observed structural

transitions in elemental materials up to now. These results have also demonstrated that a high-quality diffraction experiment is possible for the relatively low- Z elements such as phosphorus at multimegabar pressures.

II. Experimental. The high-pressure x-ray-diffraction experiment for phosphorus to 280 GPa was developed using a monochromatic x ray on the two-phase undulator beam line ID30 at the European Synchrotron Radiation Facility. A diamond-anvil cell was used for the high-pressure generation. Two experimental runs for the different anvil geometries listed in Table I were carried out in this study. A Re metal sheet with a thickness of 250 μm was preindented to a thickness of t , and holed for a sample chamber with a diameter of r . It was used as a gasket. The starting material of black phosphorus was finely ground from a single crystal with a high purity¹⁶ and packed into the sample chamber with a ruby chip. Pressure above 100 GPa was determined from the equation of state (EOS) of the Re metal.¹⁷ The estimated pressures around 100 GPa by the Re-EOS method agreed with those by the ruby fluorescence method within an error of ± 2 GPa. With the present experimental technique, the uniaxial stress may cause a systematic error in calculating the lattice constants of the sample and the Re gasket. The estimated standard deviations (esd's) for the lattice constants of the Re gasket were around 0.04–0.18% and we estimated the pressure uncertainty to be ± 2 GPa which will be described in the next section. However, the esd's for the sample

TABLE I. Geometries of diamond anvils and Re gaskets for two experimental runs; a is the top surface diameter, b is the culet diameter, β is the bevel angle of anvils, r is the sample chamber diameter, and t is the thickness of preindented Re gaskets.

Run No.	Pressure range (GPa)	Anvil geometry a - b - β (μm)-(μm)-(deg)	Gasket geometry r - t (μm)-(μm)
1	150–200	100-300-7	35-15
2	120–280	50-300-8.5	20-10

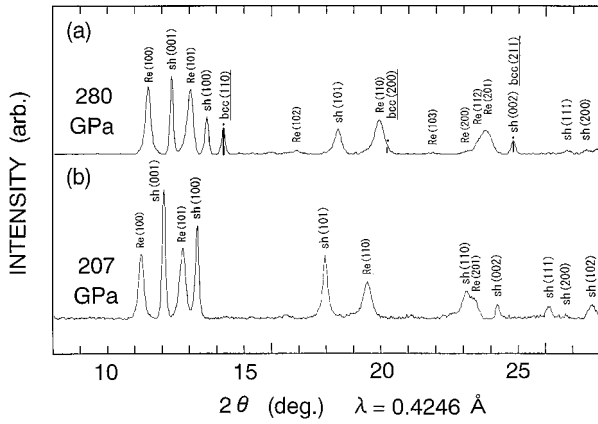


FIG. 1. The powder-diffraction patterns of the high-pressure phases of phosphorus at room temperature (a) the mixture of the sh phase, P -V, and a new high-pressure phase, P -VI at 280 GPa. In the pattern, the P -VI phase was defined as the bcc structure. (b) the sh phase at 207 GPa. Two patterns contain the diffraction peaks from the hcp-Re gasket used as the pressure marker. A background due to Compton scattering from the diamond anvils has been subtracted.

were around 0.02% and no remarkable effect of the uniaxial stress was observed. The powder patterns were obtained at room temperature by the angle-dispersive method with an image plate (IP). The monochromatic x ray of $\lambda=0.4246$ Å was focused to a beam size of $25 \times 25 \mu\text{m}^2$ with two bent mirrors. The beam was finally reduced to a size of $20 \mu\text{m}$ with a pin-hole collimator. The diffraction images were read by the Fast-Scan IP reader¹⁸ and converted to intensity vs 2θ profiles by the FIT2D software.¹⁹ In the second run the typical exposure times were 40 min.

III. Results and discussion. Figure 1(b) shows a typical diffraction pattern of the sh phase at 207 GPa in the second run. Eight diffraction peaks of the sample are observed up to $2\theta=28^\circ$ except for five peaks from the Re gasket. These data

TABLE II. The diffraction data of phosphorus at 207 GPa. The d_{obs} and I_{obs} represent the observed d values and relative intensities of the diffraction lines. The d_{cal} and I_{cal} are the calculated d values and relative intensities from the lattice constants for the sh phase and the Re gasket.

		sh of phosphorus $a = 2.1164 \pm 0.0004$ Å $c = 2.0203 \pm 0.0005$ Å			hcp of metal gasket $a = 2.498 \pm 0.001$ Å $c = 4.017 \pm 0.007$ Å	
d_{obs} (Å)	I_{obs} (%)	hkl	d_{cal} (Å)	I_{cal} (%)	hkl	d_{cal} (Å)
2.1695					100	2.167
2.0185	100	001	2.0203	46.6		
1.9070					101	1.907
1.8304	70	100	1.8329	100		
1.3576	48	101	1.3575	58.7		
1.2510					110	1.251
1.0811					200	1.083
1.0581	7	110	1.0582	8.6		
1.0443					201	1.046
1.0094	5	002	1.0101	2.1		
0.9379	4	111	0.9374	8.2		
0.9161	3	200	0.9164	3.5		
0.8851	9	102	0.8847	5.4		

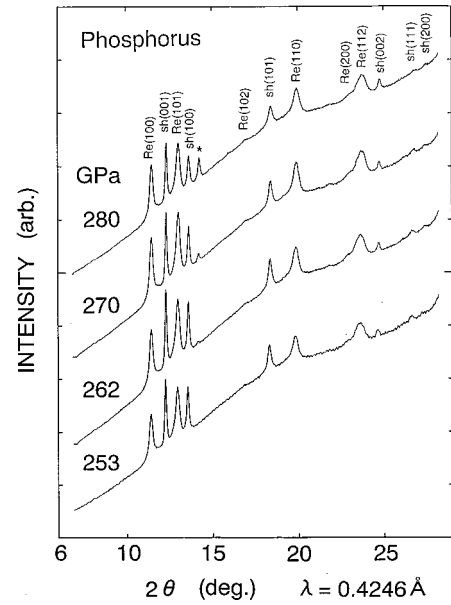


FIG. 2. The pressure dependence of the diffraction patterns of phosphorus in the higher-pressure region. A new diffraction peak, which is denoted by an asterisk (*), appears around $2\theta=14^\circ$ above 262 GPa. The result suggests that a structural transition from the sh phase to a higher-pressure phase, P -VI, occurs at 258 ± 5 GPa.

are summarized in Table II. These peaks of the sample, which have a relatively small full width at half maximum of 0.17° , were well assigned to the sh structure with a $(d_{\text{cal}} - d_{\text{obs}})/d_{\text{obs}}$ of less than 0.13%. The obtained lattice constants around 150 GPa are consistent with our previous data.³ The difference between the observed and calculated relative intensities in the table suggests the effect of preferred orientation in the sample. For the hcp-Re, lattice constants were calculated from the three strong peaks of (100), (101), and (110), and from its unit-cell volume, pressure was determined. Since the estimated error in V/V_0 was 0.08%, the uncertainty in pressure was ± 2 GPa.

With increasing pressure, the patterns suggested a structural phase transition around 262 GPa. Figure 2 shows the pressure change in the diffraction patterns in a higher pressure region. In the pattern at 262 GPa, a weak diffraction peak appears around $2\theta=14^\circ$. Upon further loading, the peak intensity increases and at 280 GPa, the maximum pressure in this study, it becomes a distinct diffraction line. The d value of the peak shows a pressure dependence and decreases from 1.724 to 1.711 Å with increasing pressure from 262 to 280 GPa. The raw diffraction image of the diffraction peak recorded on IP was a smooth Debye ring. The result suggests that a structural transition from the sh phase to a new high-pressure phase, P -VI, starts at 262 GPa and the sh phase still coexists with the P -VI phase at 280 GPa.

The pattern at 280 GPa is shown in Fig. 1(a). A background due to Compton scattering from the diamond anvils was subtracted. It would be unlikely that the number of the diffraction peak for the P -VI phase is only one in the d spacing. When compared with the pattern at 207 GPa, it was found that the diffraction peaks from the sh phase decrease in intensity. However, only the (002) peak around $2\theta=25^\circ$ increases in intensity. This suggests that a diffraction peak

TABLE III. The diffraction data of phosphorus at 280 GPa.

d_{obs} (Å)	I_{obs} (%)	sh of phosphorus $a = 2.0644 \pm 0.0004$ Å $c = 1.9755 \pm 0.0005$ Å			bcc of phosphorus $a = 2.420$ Å			hcp of metal gasket $a = 2.4526 \pm 0.0004$ Å $c = 3.941 \pm 0.007$ Å	
		hkl	d_{cal} (Å)	I_{cal} (%)	hkl	d_{cal} (Å)	I_{cal} (%)	hkl	d_{cal} (Å)
2.1226								100	2.1241
1.9753	100	001	1.9766	46.6				101	1.8697
1.8697								102	1.4444
1.7868	49	100	1.7878	100	110	1.7110	100	110	1.2263
1.7110	36							103	1.1171
1.4415								200	1.0620
1.3263	32	101	1.3259	58.7				112	1.0411
1.2264					200	1.2099	15		
1.1212									
1.0616									
1.0302	~5	110	1.0322	8.6					
1.0425									
0.9878	17	002	0.9883	2.1	211	0.9878	28		
0.9144	2	111	0.9149	8.2					
0.8942	2	200	0.8939	3.5					

from the P - VI phase superimposes on the (002) peak. The ratio of d values between the new diffraction peak and the (002) peak is 1.7321 and equals to $\sqrt{3}$. Namely both peaks may be assigned to the (110) and (211) diffraction peaks of the body-centered-cubic (bcc) structure. The expected (200) peak of the bcc structure, unfortunately, also superimposes on the (110) peak of the Re gasket. These data are summarized in Table III. The calculated lattice constants of the sh phase at 280 GPa are $a = 2.0644 \pm 0.0004$ Å, $c = 1.9755 \pm 0.0005$ Å, and $V = 7.291 \pm 0.004$ Å³. The lattice constant of the proposed bcc phase is also determined to be $a = 2.420$ Å and $V = 14.172$ Å³. The atomic volume of the bcc phase is 7.086 Å³ and consistent with the pressure vs volume relation shown in Fig. 4. This value was coincident with the theoretically predicted value of 7.05 Å³ for the bcc phase at 280 GPa (Ref. 20) (see Table IV). The estimated volume reduction, $-\Delta V$, of the transition is 0.204 Å³ and it corresponds to 2.8% of the volume at the transition pressure. These results suggest that the bcc structure is the strongest candidate for the P - VI phase. Therefore, we propose that the sh phase transforms to the bcc phase at pressure between 253 and 262 GPa. We should also add that when the new peak was assigned to the fcc or hcp structure, an impossible value in the P - V relation was given to the atomic volume. Al-

TABLE IV. Bulk modulus (B_0) and its pressure derivative (B'_0) at ambient conditions for the A17, A7, sc, sh, and bcc phases. V/V_0 denotes the relative volume of each phase extrapolated to atmospheric pressure, where $V_0(19.034$ Å³) stands for the volume of the A17 phase at atmospheric pressure.

Phase	V/V_0	B_0 (GPa)	B'_0	Ref.
A17	1.000	36 ± 2	4.5 ± 0.5	Expt. 2
A7	0.872 ± 0.01	46 ± 4	3.0 ± 0.6	Expt. 2
sc	0.815 ± 0.009	70.7 ± 0.9	4.69 ± 0.10	Expt. 3
	0.798 ± 0.01	95 ± 5	2.1 ± 0.8	Expt. 2
	0.721	127.1	4.39	Calc. 15
sh	0.746	84.1 ± 1.0	4.69	This study
bcc	0.690	108.2	3.84	Calc. 20

though the proposed bcc structure is consistent with the data and is the simplest and thus most elegant solution for all reasons discussed above, they cannot rule out the possibility of other simple structures except for fcc and hcp.

Figure 3 shows the pressure dependence of the lattice constants, a , c and c/a of the sh phase. The results of the first run agreed with those of the second runs. The lattice constant c was shorter than a by 5.2% at 137 GPa that was mentioned in our previous report.³ The present data are in good agreement with the previous results. With increasing pressure from 132 to 280 GPa, a contracts by 5.58% as does c by 4.74%. As a consequence, the c/a ratio increases from 0.948 to 0.956. The coordination number of the sh phase is 2 in the strict sense. However, the effective coordination number is 2+6 since the axial ratio is close to 1. The coordination becomes more equivalent with pressure. In this connection, since the coordination number of the bcc structure is 8, the sh to bcc transition is not contradictory to the pressure-coordination rule. The c/a ratio, with increasing pressure, initially increases and above 200 GPa, the tendency saturates. This behavior may be related to the mechanism of the

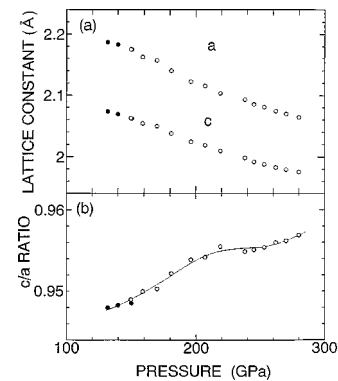


FIG. 3. The pressure dependence of the lattice constant, a and c of the sh phase, and its axial ratio, c/a . Open circles are the data obtained in the present study. Solid circles show the previous data (Ref. 3). Error bars of the data are within the data points. The solid line in the figure is a visual guide.

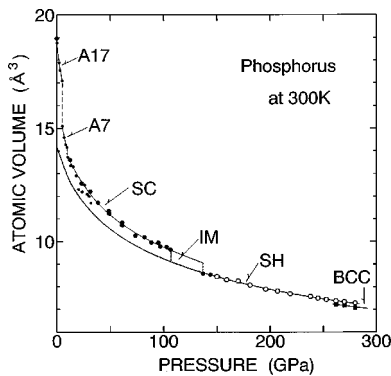


FIG. 4. The pressure dependence of the atomic volume of phosphorus up to 280 GPa. The open circles for the sh phase and solid squares for the bcc phase are the data obtained in the present study. The small solid circles show the data by Kikegawa and Iwasaki (Ref. 2) and the large solid circles are the previous data (Ref. 3). The sh to bcc transition occurs at 258 ± 5 GPa. The solid line for the sh phase represents the result of a least-squares fit of the Birch-Murnaghan equation of state, $B_0 = 84.1$ GPa, $B'_0 = 4.69$, and $V_0 = 14.2 \text{ \AA}^3$.

structural transition to the P -VI phase similar to the case of the sh phase of Si.²¹

Figure 4 shows the pressure dependence of the atomic volume together with the previous data.^{2,3} The atomic volume of the bcc phase is also plotted. At 280 GPa, it contracts to 7.08 \AA^3 and corresponds to 37.3% of 19.03 \AA^3 at normal pressure. The bulk modulus B_0 and the atomic volume V_0 of the sh phase at atmospheric pressure were estimated by fitting the P - V data with the Birch-Murnaghan equation of state.²² Since the values of the pressure derivative of the bulk modulus, B'_0 , and V_0 were highly correlated, the value of B'_0 for the sc phase,³ 4.69, was used for the fixed value of B'_0 . The B_0 was calculated by a least-squares method with the fixed value of B'_0 for various V_0 . As the result, the estimated standard deviation of observed volumes from the calculated equation of state showed a minimum of 0.0256 at $V_0 = 14.2 \text{ \AA}^3$ and $B_0 = 84.1 \pm 1.0$ GPa. The result is listed in Table IV together with those of other phases. The value of B_0 for the sh phase is larger than our previous one of the sc phase³ and this is consistent with the fact that the higher pressure phase is incompressible compared with the lower ones.

The equation of state of the sh phase of phosphorus is similar to that of the fcc phase of Si (Ref. 23) ($B_0 = 82 \pm 2$ GPa, $B'_0 = 4.22 \pm 0.05$, and $V_0 = 14.33 \pm 0.16 \text{ \AA}^3$) though the atomic volume of the sh phase is slightly larger than that of fcc-Si. The P - V curve of the bcc phase joins well that of fcc-Si. Both elements belong to the third period in the Periodic Table and these metallic high-pressure phases would behave as the so-called sp simple metal. These metals, that is, Na, Mg, Al, and Si, at the same pressure show a tendency that the smaller the ionic charge number, the larger the atomic volume. Therefore, the coincidence in the atomic volume between the bcc-P and the fcc-Si phases is an interesting result.

The present results gave the structural sequence of the pressure-induced phase transitions, that is, A17-A7-simple cubic-intermediate-simple hexagonal-bcc. The sequence is different from other group-Vb elements. However, there is a point in common with these elements such that the bcc structure occurs as the highest pressure phase. On the other hand, the simple-hexagonal phase of Si transforms to the hcp and further to the fcc phase as mentioned earlier. According to the theoretical study by McMahan and Moriarty,²⁴ the metallic high-pressure phase of phosphorus is also a natural member of third-period simple metals. The same was expected for phosphorus, but the post-simple hexagonal phase of phosphorus was the bcc and not the hcp or fcc structure. In order to understand the relative stability of the various structures based on the electronic band theory, a theoretical study is strongly desired.

IV. Conclusion. We have studied the crystal structure of phosphorus up to 280 GPa at room temperature using powder x-ray-diffraction techniques. The simple hexagonal phase, P - V , transformed to the P -VI phase at 258 ± 5 GPa. The transition pressure is the highest one for observed structural transitions in elemental materials up to now. The structure of the P -VI phase has been proposed to be the bcc structure. The equation of state of the sh phase was determined. The present data also demonstrated that a high-quality diffraction experiment is possible for relatively low- Z elements such as phosphorus at multimegabar pressures.

This work was partly supported by a Grant-in-Aid for Science Research (Grant No. 10440093) from the Ministry of Education, Science, and Culture, Japan.

- ¹J. C. Jamieson, *Science* **139**, 129 (1963).
- ²T. Kikegawa and H. Iwasaki, *Acta Crystallogr., Sect. B: Struct. Sci.* **39**, 158 (1983).
- ³Y. Akahama *et al.*, *Phys. Rev. B* **59**, 8520 (1999).
- ⁴J. Wittig and B. T. Matthias, *Science* **160**, 94 (1968).
- ⁵M. Okajima *et al.*, *Jpn. J. Appl. Phys., Part 1* **23**, 15 (1984).
- ⁶H. Kawamura *et al.*, *Solid State Commun.* **49**, 879 (1984).
- ⁷J. Wittig *et al.*, in *Solid State Physics Under High Pressure*, edited by S. Minomura (KTK Science, Tokyo, 1985), p. 217.
- ⁸H. Olijnyk *et al.*, *Phys. Lett.* **103A**, 137 (1984).
- ⁹J. Z. Hu and I. L. Spain, *Solid State Commun.* **51**, 263 (1984).
- ¹⁰Y. K. Vohra *et al.*, *Phys. Rev. Lett.* **56**, 1944 (1986).
- ¹¹M. Hanfland *et al.*, *Phys. Rev. Lett.* **82**, 1197 (1999).
- ¹²S. J. Duclos *et al.*, *Phys. Rev. Lett.* **58**, 775 (1987).
- ¹³D. Schiferl, *Phys. Rev. B* **19**, 806 (1979).
- ¹⁴K. J. Chang and M. L. Cohen, *Phys. Rev. B* **33**, 6177 (1986); **33**, 7371 (1986).
- ¹⁵T. Sasaki *et al.*, *J. Phys. Soc. Jpn.* **57**, 978 (1988).
- ¹⁶S. Endo *et al.*, *Jpn. J. Appl. Phys., Part 2* **21**, L482 (1984).
- ¹⁷Y. K. Vohra *et al.*, *Phys. Rev. B* **36**, 9790 (1987).
- ¹⁸M. Thoms *et al.*, *Nucl. Instrum. Methods Phys. Res. A* **413**, 175 (1998).
- ¹⁹A. Hammersley, computer program FIT2D, ESRF Grenoble, 1998.
- ²⁰T. Sasaki, Ph.D. thesis, Tohoku University, 1987.
- ²¹K. J. Chang and M. L. Cohen, *Phys. Rev. B* **31**, 7819 (1985).
- ²²F. Birch, *Phys. Rev.* **71**, 809 (1947).
- ²³S. J. Duclos *et al.*, *Phys. Rev. B* **41**, 12 021 (1990).
- ²⁴A. K. McMahan and J. A. Moriarty, *Phys. Rev. B* **27**, 3235 (1983).